WARSAW UNIVERSITY OF TECHNOLOGY Index 351733
FACULTY OF CIVIL ENGINEERING
COMMITTEE FOR CIVIL AND WATER ENGINEERING
POLISH ACADEMY OF SCIENCES ISSN 1230-2945
DOI: 10.24425/ace.2026.158620
ARCHIVES OF CIVIL ENGINEERING
Vol. LXXII ISSUE 2 2026
pp. 455 –466


**Research paper**

# The influence of T-stress on the stress field at the crack tip of concrete

**Shaoqing Zhou**[1]

**Abstract:** The internal structure of concrete is a three-phase material, namely matrix, aggregate, and the interface between them. Concrete, as a widely used material in engineering, its macroscopic mechanical properties and fracture characteristics are crucial for structural safety. Crack propagation is mainly caused by stress concentration near the crack tip, and T-stress, as a constant term stress near the crack tip, plays a decisive role in the crack propagation path. In this paper, the stress intensity factors of cracks near aggregate are calculated by analytical numerical method. Firstly, the contact interface between aggregate and matrix is defined as the spring layer contact interface, and then the analytical continuation method is used. Finally, an approximate analytical solution for the influence of circular aggregates on the stress intensity factor at the crack tip is obtained by calculation. The result show that the cohesive material and T-stress can influence the fracture toughness and the crack tip stress. This provided the basis for simulation of concrete fracture.

**Keywords:** concrete, aggregate, T-stress, fracture

[1]PhD., School of Civil and Environmental Engineering, Hunan University of Science and Engineering, Yongzhou, Hunan 425199, China, e-mail: 2964@huse.edu.cn, ORCID: 0000-0002-7478-9986

# 1. Introduction

As an important building material, concrete has a history of more than one hundred years, and its mechanical properties are of great concern to scientific and engineering circles. Concrete has long been regarded as a macroscopic homogeneous isotropic material, which can meet engineering requirements in general. However, it is difficult to consider the meso-composition and the complexity of the mechanical properties of concrete materials under this macroscopic assumption [1, 2]. Therefore, people have realized many advantages of studying the macroscopic damage and fracture process of concrete from the meso-scale of concrete. The combination of macro and micro research has become one of the main disciplines in recent years. Chun and Zhang [3] combine a micro- testing machine with a scanning electron microscope to reveal the secret of concrete crack propagation. Some scholars [4, 5] argue that the fracture of concrete is caused by various potential defects in the object system, and the fracture process is the process of initiation, propagation, and penetration of microcracks until macroscopic cracks lead to concrete fracture. How to study this complex mechanical problem has always been a difficult and hot spot in the field of mechanics and material science. After the emergence of fracture mechanics, academia set off an upsurge in using fracture mechanics to study concrete. Some researchers [6–8] carried out a large number of fracture tests of concrete to obtain its fracture toughness and other parameters. Concrete has long been regarded as a macroscopic homogeneous isotropic material, which can meet engineering requirements in general. However, it is difficult to consider the meso- composition and the complexity of the mechanical properties of concrete materials under this macroscopic assumption. Therefore, people have realized many advantages of studying the macroscopic damage and fracture process of concrete from the meso-scale of concrete. The combination of macro and micro research has become one of the main disciplines in recent years. Some researchers [9, 10] from the mesoscopic point of view, concrete can be regarded as a three-phase composite with cement mortar as the base phase and coarse aggregate and the bonding zone between the two as the dispersed phase.

In the research work on concrete fracture, some researchers [11, 12] participated in the path selection of cracks under the influence of nearby aggregates, and proposed the judgment criteria for the selection of crack propagation paths from theoretical and experimental perspectives. However, the stress field at the crack tip is affected by nearby aggregates, and the crack will reselect the propagation path and show a complex failure process [13]. Some experiments have shown [14] that in addition to the stress intensity factor, the non- singular stress term T-stress parallel to the crack surface can affect the crack development direction and the fracture toughness of the material. Gupta [15] believes that T-stress has many effects on fracture in various aspects. Jayadevan [16] carried out some experiments and found that T-stress affects the size of plastic area. Chen [17] found that T-stress is related to the fracture toughness of the material. Under the action of composite external load, Smith [18] studied the effect of T-stress on the deflection or bifurcation of a straight crack. Shin [19] studied the effect of T-stress of the main crack on the path stability of crack extension after deflection through perturbation analysis. Zhao [20] conducted some four-point bending tests, and the experimental results show that the introduction of T-stress is necessary to predict the initial fracture toughness of concrete under I/II composite loads. Therefore, T-stress is introduced in this paper to perform theoretical calculations on concrete fracture, providing a basis for simulating concrete fracture.

# 2. Theoretical calculation

As shown in Fig. 1, the plane infinite plate contains a circular elastic particle. The round particles are linear elastic and the contact layer and matrix are isotropic. The shear elastic moduli are $\mu_0$,$\mu_1$, and $\mu_2$, respectively. The inner contact surface and the outer contact surface are represented by curves $\Gamma_k (k = 0, 1)$ respectively.

For plane elastic problems, Stress and displacement can be expressed by two complex potentials $\varphi(z)$ and $\psi(z)$.

$$\begin{cases} 2\mu\,(u_r + iu_\theta) = e^{-i\theta}\left[\kappa\varphi(z) - \overline{z\varphi'(z)} - \overline{\psi(z)}\right] \\ \sigma_{rr} + \sigma_{\theta\theta} = 2\left[\varphi'(z) + \overline{\varphi'(z)}\right] \\ \sigma_{rr} - i\sigma_{\theta\theta} = \varphi'(z) + \overline{\varphi'(z)} - e^{2i\theta}\left[\bar{z}\varphi''(z) + \psi'(z)\right] \end{cases} \tag{2.1}$$

where:

$z = x + iy = re^{i\theta}$ is complex polar coordinates,

$\kappa = 3 - 4\nu$ is plane strain,

$\mu$ – shear modulus,

$\nu$ – Poisson's ratio.

The resultant force on arc $\overset{\frown}{AB}$ is as follows:

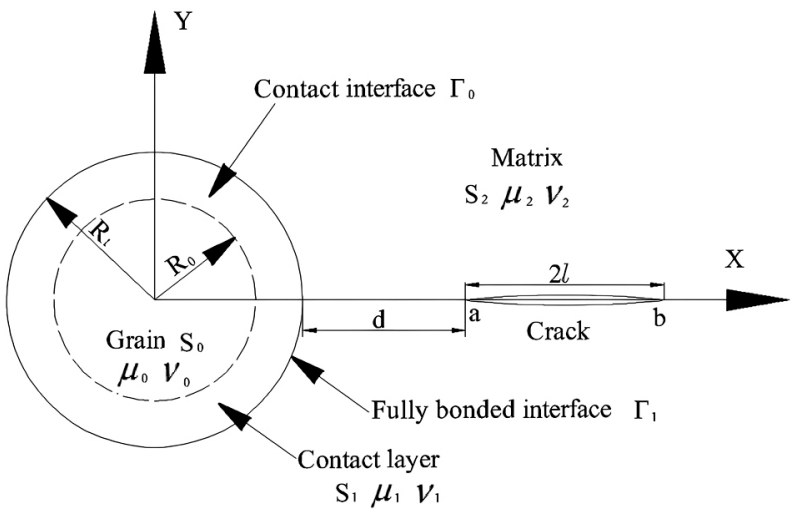


Fig. 1. Schematic diagram of three-phase material with crack

$$F_x + iF_y = -\left[\varphi(z) + \overline{z\varphi'(z)} + \overline{\psi(z)}\right]_A^B \tag{2.2}$$

where: $[f(*)]_A^B = f(A) - f(B)$ is independent of the path.

To simulate the characteristics of concrete, the contact interface between the round particles and the contact layer ($\Gamma_0$ curve) was defined in this paper due to the large difference between the properties of the aggregate and bond interface layer. At the contact interface, the force is continuously transferred, but the displacement is discontinuous at the interface. There is a gradual transition from the bonding layer in concrete to the cement mortar (i.e. the matrix), so the interface between the bonding interface layer and the matrix is a complete bonding interface (i.e. $\Gamma_1$ curve). The force and displacement in the fully bonded interface are transmitted continuously.

Yan [21] proposes a model based on the requirement that the traction force is continuous but the displacement is discontinuous when crossing the contact surface. The model assumes interface parameters of the type of spring factor, according to which the jumping change of displacement is proportional to the force at the interface. This contact interface model is often referred to as "spring layer contact interface". This paper also defines the contact surface between concrete aggregate, bond belt, and mortar as the spring layer contact interface.

The boundary conditions of the interface between circular particles and the contact layer in the curve $\Gamma_0$:

$$\|\sigma_{rr} - i\sigma_{r\theta}\| = 0, \quad \sigma_{rr} = m\,\|u_r\| - mu_r^0, \quad \sigma_{r\theta} = n\,\|u_\theta\| - nu_\theta^0, \quad z \in \Gamma_0 \tag{2.3}$$

Boundary conditions of the contact layer and the Matrix at curve $\Gamma_1$:

$$\|\sigma_{rr} - i\sigma_{r\theta}\| = 0, \quad \|u_r\| = 0, \|u_\theta\| = 0, \quad z \in \Gamma_1 \tag{2.4}$$

In Eq. (2.3), there are two contact interface parameters, $m$ and $n$ (non-negative numbers and constant along the interface). These parameters show the strength, hardness, and comprehensive bonding degree of the material interface. Saeb [22] describes these parameters in terms of simple, direct relational composition. According to Fig. 1, The parameters m and n are as follows:

$$\begin{cases} m = \dfrac{4\mu_0\mu_1}{R_0\left[\mu_0\left(\kappa_1 - 1\right) - \mu_1\left(\kappa_0 - 1\right)\right]} \\ n = \dfrac{4\mu_0\mu_1\left[3\left(\kappa_1 - 1\right)\mu_0 - 2\left(\kappa_0\mu_1 + \mu_0\right)\right]}{R_0\left\{\left[\left(\kappa_0 + 3\right)\mu_1 + \left(\kappa_1 + 3\right)\mu_0\right]\left(\mu_0 - \mu_1\right) + \left(\kappa_0\mu_1 + \mu_0\right)\left[\left(\kappa_0 - 1\right)\mu_1 - \left(\kappa_1 - 1\right)\mu_0\right]\right\}} \end{cases} \tag{2.5}$$

The expression $\|*\| = (*)_1 - (*)_0$ is the abrupt value when it crosses the interface curve $\Gamma_k (k = 0, 1)$. Especially $u^0$ is the additional displacement, which is caused by the characteristic strain $\left\{\varepsilon_x^0, \varepsilon_y^0, \varepsilon_{xy}^0\right\}$ of the particle. For example, the additional displacement can be generated when there is a temperature difference between the particle and the matrix. In Eq. (2.3), when $m = n = 0$, it will become a stress free boundary condition. If $m = n = \infty$, Eq. (2.3) will become a fully bonded consolidation interface.

Zhou [23] has studied the displacement caused by characteristic strain. According to the research results, the displacement caused by characteristic strain is expressed as follows:

$$\left(mu_r^0 - inu_\theta^0\right) = mR_0\varepsilon_1 + \left(\frac{m+n}{2R_0}\right)\left(\varepsilon_2 - i\varepsilon_3\right)z^2 + \left(\frac{m-n}{2z^2}\right)R_0^3\left(\varepsilon_2 + i\varepsilon_3\right), z \in \Gamma_0 \tag{2.6}$$

where: $\varepsilon_1 = \dfrac{\varepsilon_x^0 + \varepsilon_y^0}{2}$, $\varepsilon_2 = \dfrac{\varepsilon_x^0 - \varepsilon_y^0}{2}$, $\varepsilon_3 = \varepsilon_{xy}^0$

A simple method for solving circular boundary conditions is the series method. However, for a crack with length $2l$ in the region $S_2$, $\varphi_1(z)$ and $\psi_1(z)$ cannot be analyzed outside the curve $\Gamma_1$, so $\varphi_1(z)$ and $\psi_1(z)$ cannot be expanded into standard Laurent series in the region $S_2$. To overcome this difficulty, two new functions are introduced to represent and expand the functions into the Laurent series by using analytical continuation method. Based on Eq. (2.2) and the free boundary condition of crack surface, the following expression is obtained:

$$\begin{cases} \varphi_2(z)^+ + \left[z\overline{\varphi_2'}(z) + \overline{\psi_2'}(z)\right]^- = 0, & z \in 2l \\ \varphi_2(z)^- + \left[z\overline{\varphi_2'}(z) + \overline{\psi_2'}(z)\right]^+ = 0, & z \in 2l \end{cases} \tag{2.7}$$

Subtract the two equations in Eq. (2.7):

$$\varphi_2(z)^+ - \left[z\overline{\varphi_2'}(z) + \overline{\psi_2'}(z)\right]^+ = \varphi_2(z)^- - \left[z\overline{\varphi_2'}(z) + \overline{\psi_2'}(z)\right]^-, \quad z \in 2l \tag{2.8}$$

Define the analysis function $\Phi(z)$ in the area $S_2$

$$\Phi(z) = \varphi_2(z) - \left[z\overline{\varphi_2'}(z) + \overline{\psi_2'}(z)\right] \tag{2.9}$$

Eq. (2.8) means that $\Phi(z)$ is continuous at the crack. Therefore, $\Phi(z)$ is analytic in the region $D$. It expands into a Laurent series in the region $D$:

$$\Phi(z) = -\overline{B}z + \sum_{k=1}^{\infty} a_k z^{-k}, \quad z \in D \tag{2.10}$$

where: $a_k (k = 1, 2, \ldots)$ is an unknown complex coefficient.

Change the crack surface boundary condition Eq. (2.7) into the following form:

$$\left[\varphi_2(z) + z\overline{\varphi_2'}(z) + \overline{\psi_2'}(z)\right]^+ + \left[\varphi_2(z) + z\overline{\varphi_2'}(z) + \overline{\psi_2'}(z)\right]^- = 0 \tag{2.11}$$

Define another new analysis function $\Psi(z)$ in the region $S_2$:

$$\Psi(z) = \frac{\sqrt{(z-a)(z-b)}}{z}\left[\varphi_2(z) + z\overline{\varphi_2'}(z) + \overline{\psi_2'}(z)\right] \tag{2.12}$$

Eq. (2.11) and Eq. (2.12) show that the function $\Psi(z)$ is continuous at the crack and analytic in the region $D$. Therefore, in region d, it expands into the Laurent series:

$$\Psi(z) = \left(2A + \overline{B}\right)z + \sum_{k=1}^{\infty} b_k z^{-k}, \quad z \in D \tag{2.13}$$

where: $b_k (k = 1, 2, \ldots)$ is an unknown complex coefficient.

Now, $\varphi_2(z)$ and $\psi_2(z)$ are represented in terms of $\Phi(z)$ and $\Psi(z)$:

$$\begin{cases} \varphi_2(z) = \dfrac{z\Psi(z)}{2\sqrt{(z-a)(z-b)}} + \dfrac{\Phi(z)}{2} \\ \psi_2(z) = \overline{\varphi_2}(z) - z\varphi_2'(z) - \overline{\Phi}(z) \end{cases} \tag{2.14}$$

The complex potentials $\varphi_1(z)$ and $\psi_1(z)$ are analyzed in the interface layer (i.e. $S_1$) and expanded into the standard Laurent series:

$$\varphi_1(z) = \sum_{k=-\infty}^{\infty} d_k z^k, \quad \psi_1(z) = \sum_{k=-\infty}^{\infty} e_k z^k \tag{2.15}$$

The complex potentials $\varphi_0(z)$ and $\psi_0(z)$ are analyzed in the circular particles (i.e.$S_0$) and expanded into the Taylor series:

$$\varphi_0(z) = \sum_{k=0}^{\infty} f_k z^k, \quad \psi_0(z) = \sum_{k=0}^{\infty} g_k z^k \tag{2.16}$$

where: $d_k$, $e_k$, $f_k$ and $g_k$ are unknown complex coefficients.

By using Eq. (2.14), Eq. (2.15), and Eq. (2.16), six complex potential series forms can be obtained.

As shown in Fig. 1, the load is assumed to be uniaxial and perpendicular to the crack. Therefore, it is a mode I fracture. To obtain the stress intensity factor in the matrix crack, the following can be deduced from Eq. (2.1):

$$\begin{cases} \sigma_{xx} = Re\left[\overline{\varphi_2'(z)} + \varphi_2'(z) - z\overline{\psi_2''(z)} - \overline{\psi_2'(z)}\right] \\ \sigma_{xy} = Im\left[\overline{\varphi_2'(z)} + \varphi_2'(z) - z\overline{\psi_2''(z)} - \overline{\psi_2'(z)}\right] \\ \sigma_{yy} = Re\left[\overline{\varphi_2'(z)} + \psi_2'(z) + z\overline{\psi_2''(z)} + \overline{\psi_2'(z)}\right] \end{cases} \tag{2.17}$$

By substituting the Eq. (2.14) into Eq. (2.17), the stress of mode I fracture at the point a is obtained:

$$\begin{cases} \sigma_{xx} = -\dfrac{2a\sigma^{\infty}}{\sqrt{2lr_1}}\left(\dfrac{3}{8}\sin\dfrac{\theta_1}{2} + \dfrac{1}{8}\sin 5\dfrac{\theta_1}{2}\right)\left[1 - \dfrac{1}{2a\sigma^{\infty}}\displaystyle\sum_{k=1}^{\infty} k b_{k+1} a^{-(k+1)}\right] \\ \qquad\qquad - \sigma^{\infty}\left[1 - \dfrac{1}{2a\sigma^{\infty}}\displaystyle\sum_{k=1}^{\infty} k b_{k+1} a^{-(k+1)}\right] + O(r_1) \\ \sigma_{yy} = -\dfrac{2a\sigma^{\infty}}{\sqrt{2lr_1}}\left(\dfrac{5}{8}\sin\dfrac{\theta_1}{2} - \dfrac{1}{8}\sin 5\dfrac{\theta_1}{2}\right)\left[1 - \dfrac{1}{2a\sigma^{\infty}}\displaystyle\sum_{k=1}^{\infty} k b_{k+1} a^{-(k+1)}\right] + O(r_1) \\ \sigma_{xy} = -\dfrac{2a\sigma^{\infty}}{\sqrt{2lr_1}}\left(\dfrac{1}{8}\cos\dfrac{\theta_1}{2} - \dfrac{1}{8}\cos 5\dfrac{\theta_1}{2}\right)\left[1 - \dfrac{1}{2a\sigma^{\infty}}\displaystyle\sum_{k=1}^{\infty} k b_{k+1} a^{-(k+1)}\right] + O(r_1) \end{cases} \tag{2.18}$$

where: $z - a = r_1 e^{i\theta_1}$ $(0 \le \theta_1 \le 2\pi)$.

When $\theta_1 = 0$, the T-stress at point a can be obtained using the stress difference method:

$$T = \lim_{r\to 0}\left(\sigma_{xx} - \sigma_{yy}\right) = -\sigma^{\infty}\left[1 - \frac{1}{2a\sigma^{\infty}}\sum_{k=1}^{\infty} k b_{k+1} a^{-(k+1)}\right] \tag{2.19}$$

The content in the square brackets of Eq. (2.18) and Eq. (2.19) shows the effects of the stress intensity factor and T-stress corresponding to spherical particles and the contact interface.

## 3. Calculation and analysis of cohesion effect on fracture

In this paper, it is considered that the contact layer is isotropic and vertical, which is equal to the tangential spring factor contact surface parameters(i.e. $m = n$). The contact surface which has the same influence on the vertical direction and the tangent direction is called the spring layer contact surface. Let's set a dimensionless $X = \dfrac{mR_0}{\mu_1}$, which describes the degree of interfacial bonding. When the $X$ value is very small, the contact surface is very loose. When the $X$ value is very large, the contact surface approaches to the fully bonded interface. In this paper, the Poisson ratios are assumed to be $\nu_0 = \nu_1 = \nu_2 = 0.3$. Their shear elastic moduli are $\mu_0$,$\mu_1$ and $\mu_2$ respectively.

The crack point a is closer to the particle than point b and is more affected by the particle. Therefore, this paper mainly studies the stress intensity and T-stress at point a.

According to the maximum circumferential stress fracture criterion

$$(\sigma_{\varphi\varphi})_{\max} = (\sigma_{\varphi\varphi})_c \tag{3.1}$$

According to the derivation of Zhou [24], we get

$$\sqrt{2\pi r}\,(\sigma_{\varphi\varphi})_c = \cos\frac{\varphi}{2}\left[K_I\cos^2\frac{\varphi}{2} - \frac{3}{2}K_{II}\sin\varphi\right] + \sqrt{2\pi r}T\sin^2\varphi \tag{3.2}$$

Let $K_e = \sqrt{K_I^2 + K_{II}^2}$, and introduce dimensionless: $C = \dfrac{T}{K_e}\sqrt{2\pi r}$

Then Eq. (3.2) becomes:

$$\frac{\sqrt{2\pi r}\,(\sigma_{\phi\phi})_c}{K_e} = \cos\frac{\phi}{2}\left[\frac{K_I}{K_e}\cos^2\frac{\phi}{2} - \frac{3}{2}\frac{K_{II}}{K_e}\sin\phi\right] + C\sin^2\phi \tag{3.3}$$

Then Eq. (3.3) is the maximum circumferential stress fracture criterion after adding T-stress.

Taking the interface parameter $X = 1$ and the elastic modulus $\mu_0 : \mu_1 : \mu_2 = 4 : 1 : 1$ (i.e. the internal particle stiffness is large), the relationship between the stress at point a of the crack and the T-stress and distance is obtained from Eq. (3.3) in Fig. 2. The parameter $\dfrac{\sqrt{2\pi r_c}\,(\sigma_{\phi\phi})_c}{K_e}$ of the coordinate axis in Fig. 2 describes the stress at point a, the parameter $C$ describes the magnitude of T-stress, and the parameter $\dfrac{r}{R_1}$ describes the distance from the crack point a to the particle. From Fig. 2, it can be seen that in the $\dfrac{\sqrt{2\pi r_c}\,(\sigma_{\phi\phi})_c}{K_e}$ axis and $C$ axis directions, as the T-stress decreases, the circumferential stress $\sigma_{\theta\theta}$ at the crack tip also decreases accordingly. In the $\dfrac{\sqrt{2\pi r_c}\,(\sigma_{\phi\phi})_c}{K_e}$ axis and $\dfrac{r}{R_1}$ axis directions, as the distance increases, the circumferential stress $\sigma_{\theta\theta}$ at the crack tip sharply decreases.

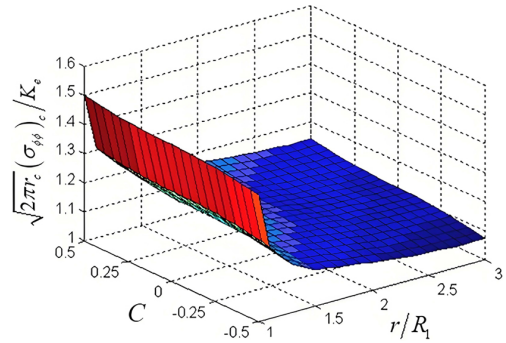


Fig. 2. Variation of stress at crack point a with T-stress and distance when internal particle stiffness is large

Take the interface parameter $X = 1$, change the elastic modulus of the particles $\mu_0 : \mu_1 : \mu_2 = 0.25 : 1 : 1$ (i.e. lower internal particle stiffness), and obtain Fig. 3 from Eq. (3.3). Comparing Fig. 2 and Fig. 3, it can be seen that when the stiffness of the particles is changed, the circumferential stress at the crack tip is also affected, and its value is slightly smaller than the circumferential stress at the crack tip of the particles with large stiffness. Therefore, compared with the case of particles with higher stiffness and particles with lower stiffness in the matrix, particles with higher stiffness will make it easier for cracks to propagate. In the $\dfrac{\sqrt{2\pi r_c}\,(\sigma_{\phi\phi})_c}{K_e}$ axis and $C$ axis directions, as the T-stress decreases, the circumferential stress $\sigma_{\theta\theta}$ at the crack tip also decreases slightly. In the $\dfrac{\sqrt{2\pi r_c}\,(\sigma_{\phi\phi})_c}{K_e}$ axis and $\dfrac{r}{R_1}$ axis directions, as the distance increases, the circumferential stress $\sigma_{\theta\theta}$ at the crack tip also sharply decreases.

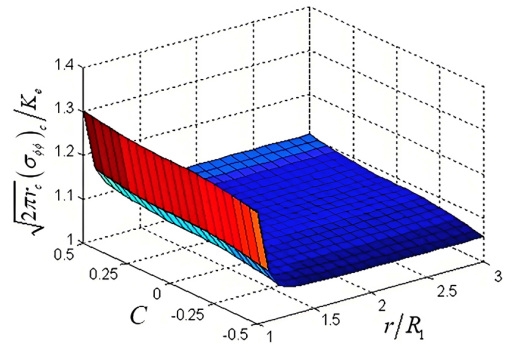


Fig. 3. Variation of stress at crack point a with T-stress and distance when internal particle stiffness is small

Take the elastic modulus $\mu_0 : \mu_1 : \mu_2 = 1 : 1 : 1$ (i.e. the stiffness is the same), increase the interface parameter $X = 10$, and obtain Fig. 4 from Eq. (3.3). In the direction of $\dfrac{\sqrt{2\pi r_c}\,(\sigma_{\phi\phi})_c}{K_e}$ axis and $\dfrac{r}{R_1}$ axis, the circumferential stress $\sigma_{\theta\theta}$ at the crack tip also decreases as the crack

approaches the particle. This shows that the contact layer with high stiffness can restrain the crack growth and reduce the stress intensity at the crack tip. In the direction of $\frac{\sqrt{2\pi r_c}\,(\sigma_{\phi\phi})_c}{K_e}$ axis and $C$ axis, with the decrease of T-stress, the circumferential stress $\sigma_{\theta\theta}$ at the crack tip also decreases a little.

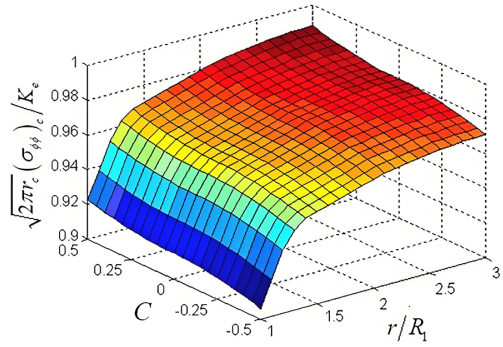


Fig. 4. Variation of stress at crack point a with T-stress and distance when the stiffness of contact layer is large

Take the elastic modulus $\mu_0 : \mu_1 : \mu_2 = 1 : 1 : 1$ (i.e. the stiffness is the same), reduce the interface parameter $X = 0.1$, and obtain Fig. 5 from Eq. (3.3). In the direction of $\frac{\sqrt{2\pi r_c}\,(\sigma_{\phi\phi})_c}{K_e}$ axis and $\frac{r}{R_1}$ axis, the circumferential stress $\sigma_{\theta\theta}$ at the crack tip increases as the crack approaches the particle. This shows that the contact layer with small stiffness can not restrain the crack growth, and increases the stress intensity at the crack tip. In the direction of $\frac{\sqrt{2\pi r_c}\,(\sigma_{\phi\phi})_c}{K_e}$ axis and $C$ axis, with the decrease of T-stress, the circumferential stress $\sigma_{\theta\theta}$ at the crack tip also decreases a little.

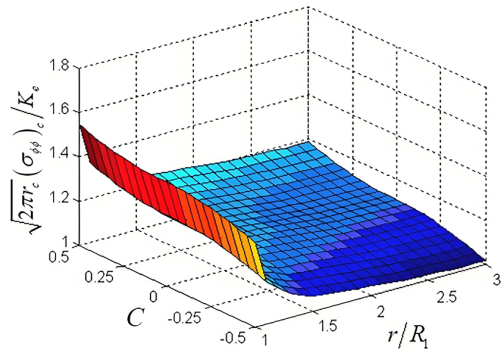


Fig. 5. Variation of stress at crack point a with T-stress and distance when the stiffness of the contact layer is small

# 4. Conclusions

In this paper, when conducting theoretical calculations on the fracture of three-phase material concrete, the T-stress and stress strength factors at the crack tip were solved using series expansion. The calculation results show that the properties of the cohesive and T-stress affect the fracture toughness and the stress at the crack tip, which provides a basis for simulating concrete fracture.

Based on this study, the following conclusions can be drawn:

1. The inclusion of particles has a greater influence on the stress intensity factor near the crack tip of aggregate, but has no significant effect on the far of the crack tip. On the other hand, as the distance between cracks and particles increases, the stress effect of particles on the crack tip decreases gradually.
2. When the interfacial parameter $X$ $\left(X = \dfrac{mR_0}{\mu_1}\right)$, which describes the degree of interfacial bonding) is small, the presence of particles with high stiffness in the matrix will make the crack propagate more easily than the absence of particles. For the case of high interfacial parameter value $X$, due to the shielding effect of the contact interface (spring layer), although the particle stiffness is high, there is no significant influence on the crack growth.
3. When the particle stiffness is smaller than that of the surrounding material, the stress intensity factor increases rapidly as the crack tip approaches the interfacial layer, which makes the crack easy to propagate.
4. The contact layer with high stiffness has shielding effect, which reduces the stress strength at the crack tip. When the stiffness of the contact layer is small, the stress intensity factor will increase rapidly and the crack will develop easily when the crack tip is close to the interface layer.
5. The calculation results in this paper show that T-stress has an influence on the circumferential stress at the crack tip. When the T-stress is negative, it can reduce the circumferential stress at the crack tip, thereby increasing the fracture toughness. Zhao [20] proposed that negative T-stress can enhance the fracture toughness of concrete. The calculation results of this article are consistent with their experimental results.

## References

[1] Z. Yan, H. Ge, S. Guo, X. Wu, and G. Zhao, "Flexural strength test and meso-mechanical evolution behavior of cement concrete based on discrete element method", *Computational Particle Mechanics*, vol. 9, no. 1, pp. 85–99, 2022, doi: 10.1007/s40571-021-00395-0.

[2] L. Zhu, F. Dang, Y. Xue, W. Ding, and L. Zhang, "Comparative study on the meso-scale damage evolution of concrete under static and dynamic tensile loading using X-ray computed tomography and digital image analysis", *Construction and Building Materials*, vol. 250, art. no. 118848, 2020, doi: 10.1016/j.conbuildmat.2020.118848.

[3] C. Chun, Y. Zhang, R. Wang, and J. Yang, "Application of micro-structure testing in the analysis of the cause of concrete cracks", *Key Engineering Materials*, vol. 629-630, pp. 121–129, 2014, doi: 10.4028/www.scientific.net/KEM.629-630.121.

[4] B. Wu, Z. Li, K. Tang, and K. Wang, "Microscopic multiple fatigue crack simulation and macroscopic damage evolution of concrete beam", *Applied Sciences*, vol. 9, no. 21, art. no. 4664, 2019, doi: 10.3390/app9214664.

[5] S. Khalilpour, E. BaniAsad, and M. Dehestani, "A review on concrete fracture energy and effective parameters", *Cement and Concrete Research*, vol. 120, pp. 294–321, 2019, doi: 10.1016/j.cemconres.2019.03.013.

[6] L. Xiong, H. Chen, Z. Xu, and D. Hu, "Uniaxial compression test and numerical simulation of rock-like specimen with T-Shaped cracks", *Archives of Civil Engineering*, vol. 69, no. 2, pp. 227–244, 2023, doi: 10.24425/ace.2023.145265.

[7] J. Guan, Q. Li, Z. Wu, and S. Zhou, "Initial fracture toughness of site-casting dam concrete", *Journal of Hydraulic Engineering*, vol. 45, no. 12, pp. 1487–1492, 2014, doi: 10.13243/j.cnki.slxb.2014.12.013.

[8] S. Yang, M. Wang, T. Lan, S. Liu, and Z. Sun, "Fracture model for predicting tensile strength and fracture toughness of concrete under different loading rates", *Construction and Building Materials,* vol. 365, art. no. 129978, 2014, doi: 10.1016/j.conbuildmat.2022.129978.

[9] K. Kim and L.J. Sudak, "Interaction between a radial matrix crack and a three-phase circular inclusion with imperfect interface in plane elasticity", *International Journal of Fracture*, vol. 131, no. 2, pp. 155-172, 2005, doi: 10.1007/s10704-004-3636-6.

[10] C. Shi, Q. Tu, H. Fan, and S. Li, "An interphase model for effective elastic properties of concrete composites", *Journal of Micromechanics and Molecular Physics*, vol. 1, no. 1, art. no. 1650005, 2016, doi: 10.1142/S2424913016500053.

[11] P. Chaudhuri, "Multi-scale modeling of fracture in concrete composites", *Composites Part B: Engineering,* vol. 47, pp. 162–172, 2013, doi: 10.1016/j.compositesb.2012.10.021.

[12] Ł. Skarżyński, M. Nitka, and J. Tejchman, "Modelling of concrete fracture at aggregate level using FEM and DEM based on X-ray $\mu$CT images of internal structure", *Engineering Fracture Mechanics,* vol. 147, pp. 13–35, 2015, doi: 10.1016/j.engfracmech.2015.08.010.

[13] H. Haeri, "Simulating the Crack Propagation Mechanism of Pre-Cracked Concrete Specimens Under Shear Loading Conditions", *Strength of Materials*, vol. 47, no. 4, pp. 618–632, 2015, doi: 10.1007/s11223-015-9698-z.

[14] Y. Ueda, K. Ikeda, T. Yao, and M. Aoki, "Characteristics of Brittle Fracture Under General Combined Modes Including Those Under Biaxial Tensile Loads", *Engineering Fracture Mechanics,* vol. 18, no. 6, pp. 1131-1158, 1983, doi: 10.1016/0013-7944(83)90007-3.

[15] M. Gupta, R.C. Alderliesten, and R. Benedictus, "A review of T-stress and its effects in fracture mechanics", *Engineering Fracture Mechanics*, vol. 134, pp. 218–241, 2015, doi: 10.1016/j.engfracmech.2014.10.013.

[16] K.R. Jayadevan, R. Narasimhan, T.S. Ramamurthy, and B. Dattaguru, "Effect of T-stress and loading rate on crack initiation in rate sensitive plastic materials", *International Journal of Solids & Structures*, vol. 39, no. 7, pp. 1757–1775, 2002, doi: 10.1016/S0020-7683(02)00012-4.

[17] Y.Z. Chen, "Closed form solutions of T-stress in plane elasticity crack problems", *International Journal of Solids and Structures*, vol. 37, no. 11, pp. 1629–1637, 2000, doi: 10.1016/S0020-7683(98)00312-6.

[18] D.J. Smith, M.R. Ayatollahi, and M.J. Pavier, "The role of T-stress in brittle fracture for linear elastic materials under mixed-mode loading", *Fatigue & Fracture of Engineering Materials & Structures*, vol. 24, no. 2, pp. 137–150, 2001, doi: 10.1046/j.1460-2695.2001.00377.x.

[19] K.S. Dong and J.J. Lee, "Numerical analysis of dynamic T-stress of moving interfacial crack", *International Journal of Fracture*, vol. 119, no. 3, pp. 223–245, 2003, doi: 10.1023/A:1023956215025.

[20] Y. Zhao, W. Dong, B. Xu, and J. Liu, "Effect of T-stress on the initial fracture toughness of concrete under I/II mixed-mode loading", *Theoretical and Applied Fracture Mechanics,* vol. 96, pp. 699–706, 2018, doi: 10.1016/j.tafmec.2017.10.009.

[21] J. Yan, J. Zhu, and L. Ma, "Analytical solutions for coated circular inhomogeneity with non-uniform axisymmetric eigenstrain distribution", *International Journal of Solids and Structures*, vol. 243, art. no. 111567, 2022, doi: 10.1016/j.ijsolstr.2022.111567.

[22] S. Saeb, S. Firooz, P. Steinmann, and A. Javili, "Generalized interfaces via weighted averages for application to graded interphases at large deformations", *Journal of the Mechanics and Physics of Solids,* vol. 149, art. no. 104234, 2021, doi: 10.1016/j.jmps.2020.104234.

[23] K. Zhou, et al., "A review of recent works on inclusions", *Mechanics of Materials*, vol. 60, pp. 144–158, 2013, doi: 10.1016/j.mechmat.2013.01.005.

[24] S. Zhou, S. Guo, and X. Li, "T-stress's impact on rock's fracture toughness and propagation path", *Journal of Central South University of Technology,* vol. 40, pp. 797–802, 2009.

Received: 2025-03-10, Revised: 2025-04-01